

# Indirect sensitivity to $Z$ 's in high-energy $e^+e^-$ collisions: a “standard” vs. “composite” study

Marco Battaglia\*

*University of California at Santa Cruz and  
Lawrence Berkeley National Laboratory,  
Berkeley, CA - USA and  
CERN, Geneva, Switzerland*

Francesco Coradeschi<sup>†</sup> and Daniele Dominici<sup>‡</sup>

*Università degli Studi di Firenze, Dipartimento di Fisica,  
Firenze - Italy and Istituto Nazionale di Fisica Nucleare, Sezione di Firenze - Italy*

Stefania De Curtis<sup>§</sup>

*Istituto Nazionale di Fisica Nucleare, Sezione di Firenze - Italy*

(Dated: June 20, 2011)

## Abstract

We compare the phenomenology of two models, the so-called “minimal  $Z'$ ” and an effective model an SM-like Higgs is realised as a composite state of a new strong interaction, at a multi-TeV linear collider in the hypothesis that the new physics is at a scale beyond the direct reach of the machine.

PACS numbers: 13.66.Fg, 14.80.Cp

---

\* MBattaglia@lbl.gov

† coradeschi@fi.infn.it

‡ dominici@fi.infn.it

§ decurtis@fi.infn.it

## I. INTRODUCTION

Additional heavy neutral gauge bosons appear in many extensions of the Standard Model (SM). Current limits from direct searches at hadron colliders constrain their mass to be above  $\sim 1.5$  TeV [1, 2], where the limit depends on the assumed  $Z'$  couplings. The LHC will further improve these limits, up to and possibly beyond, masses of order of the anticipated centre-of-mass energy of a lepton collider. However, even if no signal is observed at the LHC an high energy lepton collider, such as the ILC and especially CLIC, may still be sensitive to the existence of an heavy  $Z'$  boson. Precision electroweak observables are in fact sensitive to the effects of new particles at mass scales well above the collision center-of-mass energy ( $\sqrt{s}$ ).

In this work, we compare the phenomenology of two different models, both containing  $Z'$  bosons, at an  $e^+e^-$  collider and in the hypothesis that the scale of new physics is beyond the direct reach of the machine, by analyzing electroweak precision observables in  $e^-e^+ \rightarrow f\bar{f}$  processes. The first model is the so-called “minimal  $Z'$ ” [3] (see also [4]), in which it is assumed that some new physics at a very high energy scale (perhaps as high as the grand unification scale) only manifests itself at the TeV scale through a single  $Z'$ . In the second model, first studied in [5], the Higgs field (along with several other fields, including three  $Z'$ s) is realised as a composite state from a strong interaction at the TeV scale; for easy of reference, in the following we refer to this model as Effective Composite Higgs Model (ECHM). These models depict completely different physical situations and each represents one of the simplest realizations of the corresponding scenario, so they are well-suited to be used as tests of a collider sensitivity.

The work is organised as follows. In section II we discuss the details of the analysis. In section III we present the models and show results for electroweak observables, then summarizing our conclusions.

## II. ANALYSIS SET-UP

We study the case of a 3 TeV collider with beam polarisation, and consider  $f\bar{f}$  production, with  $f = \mu, t$ . This choice of final states highlights the difference between the  $Z'$  model and the ECHM. In the former, the sensitivity to muons and  $t$  quarks is comparable, while in the

latter, the sensitivity to the  $t$  is much enhanced.

### A. Observables

In the SM,  $e^-e^+ \rightarrow f\bar{f}$  processes can be fully parametrized in terms of four helicity amplitudes, which can be in turn determined by measuring four observables: the total production cross section,  $\sigma_{f\bar{f}}$ , the forward-backward asymmetry  $A_{FB}$ , the left-right asymmetry,  $A_{LR}$ , and the polarized forward-backward asymmetry,  $A_{FB}^{pol}$ . These observables still characterize the  $e^-e^+ \rightarrow f\bar{f}$  process if  $Z'$ 's are the only new neutral state; in fact, in the case of a single  $Z'$  of known mass (that is, if an high-mass  $Z'$  candidate is observed at the LHC), they can be used to determine the new vector couplings to both  $e$  and  $f$  up to a sign ambiguity [12]. Note that the relative uncertainties on  $A_{LR}$  and  $A_{FB}^{pol}$  depend on the relative uncertainty on the effective beam polarisation:

$$\frac{\Delta_{pol}A_{LR}}{A_{LR}} = \frac{\Delta_{pol}A_{FB}^{pol}}{A_{FB}^{pol}} = \frac{\Delta P_{eff}}{P_{eff}}, \quad P_{eff} = \frac{P_{e^-} - P_{e^+}}{1 + P_{e^-}P_{e^+}}, \quad (1)$$

where  $P_{e^-}(P_{e^+})$  gives the degree of polarisation of the  $e^-(e^+)$  beam, with  $P_{e^-} = -1$  meaning a fully left polarized and  $P_{e^+} = +1$  a fully right polarized beam. In absence of beam polarisation only the first two observables are available.

### B. Details of the Calculation

Our analysis has been performed using the CalcHEP [6] package. The model files for the ECHM model have been generated from the Lagrangian using the FeynRules [7] package in Mathematica [8], and its couplings have been calculated by implementing an external C library to obtain a numerical diagonalization of the mass matrices. While CalcHEP generates matrix elements at tree level, it can be set to incorporate corrections from Initial State Radiation (ISR) and beamstrahlung, which are known to be significant at an high-energy linear collider. ISR is implemented using the formalism of [9]. The beamstrahlung uses the CLIC parameters adopted for the CDR [11]: horizontal beam size: 45 nm, vertical beam size: 1 nm, bunch length: 44  $\mu\text{m}$ , particles per bunch:  $3.7 \cdot 10^9$ .

A cut on the polar angle of the final state fermions has been imposed at  $|\cos\theta| < 0.9$  to ensure the observability of final fermions in the detector, and also a cut in final state

energy,  $E_{f,\bar{f}} > 0.8 E_{beam}$ , to select “pure” high energy events, that is events that have not experienced large energy loss from ISR and beamstrahlung. As shown in fig. 1, this ensures that the corrected cross-section is within  $\sim 10\%$  of the Born one.

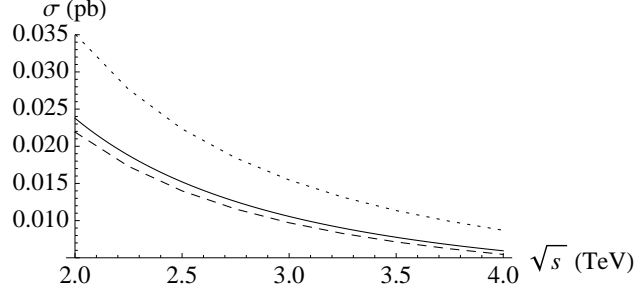


FIG. 1. Cross section for the  $e^+e^- \rightarrow \mu^+\mu^-$  in the SM at the Born level (solid line), with ISR and beamstrahlung with no cuts (dotted line), and with ISR, beamstrahlung and the cut  $E_{f,\bar{f}} > 0.8 E_{beam}$  (dashed line). The cut selects final state fermions which did not lose much energy to radiation, bringing the cross-section within 5 – 10% of the Born value.

### C. Sensitivity scaling law

In the indirect limit in which the mass scale of NP is much greater than the center-of-mass energy of the collider, sensitivity to NP is dominated by interference with the SM, which leads to a shift in the observables of the form

$$\Delta\mathcal{O} \propto g_X^2/M_{Z'_X}^2 + O(s/M_{Z'_X}^2), \quad (2)$$

with  $\mathcal{O}$  a generic observable and  $g_X$ ,  $M_{Z'_X}$  generic coupling and mass scale of the  $Z'$  model respectively. Since the statistical uncertainty scales as  $\sqrt{L_{int}} s$  with integrated luminosity, this leads to the sensitivity scaling law:

$$M_{Z'_X}/g_X \propto (L_{int} s)^{1/4} \quad (3)$$

if the uncertainty is statistic-dominated, which is a safe assumption at least in the case of asymmetries. As already noted, a potential exception are  $A_{LR}$  and  $A_{FB}^{pol}$  which are affected by the systematic uncertainty on the degree of beam polarisation.

### III. RESULTS

We present the results of our analysis by giving deviations of the observables listed in section II with respect to the SM for the two chosen models, in function of the model parameters. We plot the relative deviation  $\delta\sigma/\sigma^{SM}$  of the cross-section and the absolute deviation  $\delta A_X$  of the asymmetries ( $\delta\mathcal{O} = \mathcal{O}^{NP} - \mathcal{O}^{SM}$  for every observable  $\mathcal{O}$  and  $A_X$  is a generic asymmetry).

Before discussing the results for the two models adopted for this study, it is useful and instructive to show the deviations in function of the  $Z'$  mass in the so-called Sequential SM (SSM), which includes a  $Z'$  by replicating the SM couplings to fermions of the  $Z^0$  for the new state. The SSM is not a realistic model, but it is useful as a benchmark and serves to illustrate the mass scaling of the observable deviations (2), which follows a similar pattern also in every  $Z'$  model. Deviations are shown in fig. 2.

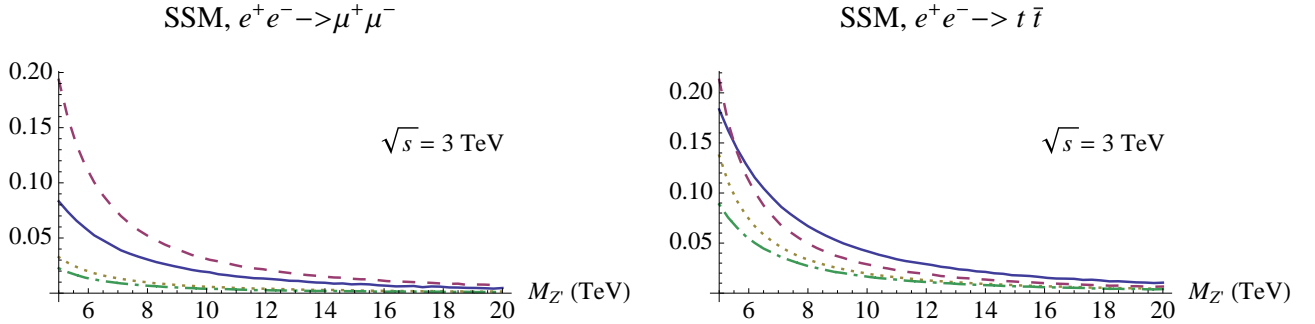


FIG. 2. Deviations with respect to the SM for  $e^+e^- \rightarrow \mu^+\mu^-$  (left) and to  $e^+e^- \rightarrow t\bar{t}$  (right) in the SSM model at  $\sqrt{s}=3$  TeV. The continuous line represents the relative cross-section deviation  $\delta\sigma/\sigma^{SM}$ ; the dashed line gives  $\delta A_{FB}$ , the dotted line  $\delta A_{LR}$  and the dot-dashed line  $\delta A_{FB}^{pol}$ .

#### A. Minimal $Z'$ model

"Minimal  $Z'$ " is a semi model-independent parametrization of a light  $Z'$  and its couplings, first proposed in [3]. The model phenomenology at LHC has been recently studied in [4]. The basic assumption of the description is the presence of a single new vector boson state with a mass of order TeV plus the *minimum amount* of extra non-SM fields needed to make the model renormalisable and anomaly-free, hence the adjective "minimal".

This approach automatically takes into account effects from the *most general possible* kinetic and mass mixings; a  $Z - Z'$  mixing is automatically induced, and the mixing angle  $\theta'$  is defined in terms of the free parameters of the model (see [3] for details). Before the mixing, the coupling of the  $Z'$  to fermions can be written as:

$$\mathcal{L}_{int}^{Z'} = ig_Z Z'_\mu \bar{f} \gamma^\mu (\tilde{g}_Y Y + \tilde{g}_{BL}(B - L)) f, \quad (4)$$

where  $g_Z$  is the standard  $Z$  coupling, and  $Y$ ,  $B$  and  $L$  are the usual hypercharge, baryon and lepton numbers. The model has thus three free parameters: the  $Z'$  mass  $M_{Z'}$  and the couplings  $\tilde{g}_Y$  and  $\tilde{g}_{BL}$  (in fact, the theory has  $N - 1$  additional free parameters, which fix the couplings of the  $Z'$  to the  $N$  right-handed neutrinos  $N_R^i$ ; for general values of  $\tilde{g}_Y$  and  $\tilde{g}_{BL}$ , at least *three* heavy neutrinos are needed to cancel anomalies. However, these are irrelevant at low energy if one chooses -as it is customary - the mass of the  $N_R^i$  to be greater than  $M_{Z'}/2$ ). The  $Z'$ -Higgs coupling is equal to  $g_Z \tilde{g}_Y$ .

Several well-known simple  $Z'$  models can be reproduced in this framework by fixing the ratio  $\tilde{g}_Y/\tilde{g}_{BL}$  [3, 4] (for instance the  $B - L$  and the  $E_{6-\chi}$  models). However, the whole of the model parameter space is potentially interesting. Since there are no theoretical reasons to predict a particularly large value for the couplings, we have restricted the analysis to the region  $|\tilde{g}_Y|, |\tilde{g}_{BL}| < 1$ , which is enough to clearly illustrate the model behaviour. Also, for the sake of brevity we only show results for a fixed value of the  $Z'$  mass,  $M_{Z'} = 5$  TeV; for higher mass values, deviations scale in a similar way as the one shown in fig. 2 for the SSM. Our results are shown in figs. 3 and 4. Similarly to what happens in the benchmark model SSM, both fermion channels display a similar sensitivity. Furthermore, deviations are very significant, being  $> 10\%$  in the majority of the parameter space for all observables. using the scaling of eq. (3), masses well above 10 TeV can be accessed, if precise enough measurements are available.

## B. Effective Composite Higgs Model

The second scheme we discuss here, first proposed in [5], is based on the deconstruction of an extra-dimensional scenario.

The model includes two four-dimensional sectors connected by mass mixing. The first, the "elementary" sector, is an  $SU(3) \otimes SU(2)_L \otimes U(1)_Y$  SM-like gauge theory, with the

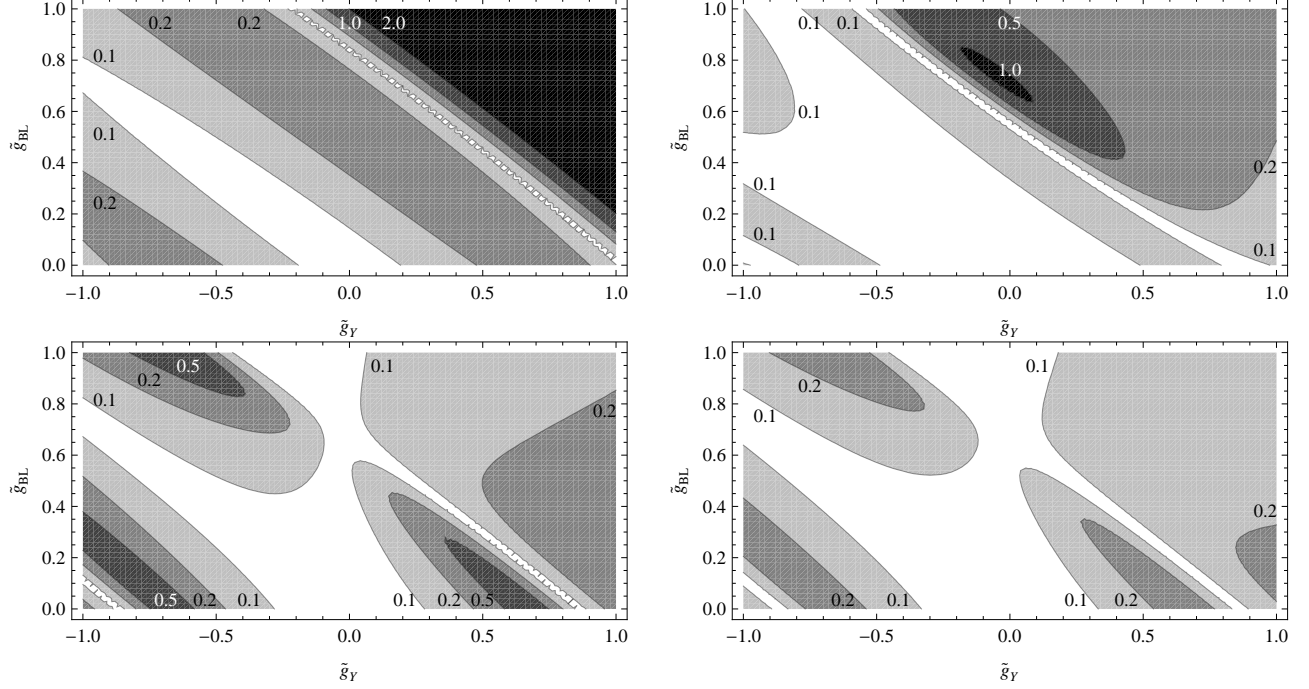


FIG. 3. Deviations with respect to the SM for  $e^+e^- \rightarrow \mu^+\mu^-$  in the minimal  $Z'$  model at  $\sqrt{s}=3$  TeV. In the upper row we show  $|\delta\sigma|/\sigma^{SM}$  and  $|\delta A_{FB}|$ , and in the lower row the absolute value for the deviations of the polarisation-based observables  $A_{LR}$  and  $A_{FB}^{pol}$ . Darker region imply larger deviations, and contour lines correspond to the printed fixed deviation values. The middle of the X-axis corresponds to  $\tilde{g}_Y = \tilde{g}_{BL} = 0$ , that is, to the SM.

usual fermion content (plus right-handed neutrinos to help generate neutrino masses) but no Higgs and no mass terms. The second is an effective description of a composite sector via an  $SU(3)_* \otimes SU(2)_L \otimes SU(2)_R \otimes U(1)_X$  gauge theory, explicitly broken by the insertion of mass terms and including a scalar (Higgs) bi-doublet and an expanded fermion sector.

The free parameters of the model, which are relevant for the analysis, are:

- in the gauge sector, two composite gauge couplings,  $g^{*(1,2)}$ , which we have for simplicity chosen to be equal to a common value  $g^*$ , and a composite gauge boson mass scale  $M^*$  (the gauge couplings in the elementary sector have to be fixed in order to reproduce the SM at low energy);
- the fermion sector has many parameters: we have 18 mixing angles, one for each left-handed  $SU(2)_L$  doublet and right-handed singlet in the SM plus three right-handed neutrinos; the Yukawa parameters, described by four complex  $3 \times 3$  matrices; and the

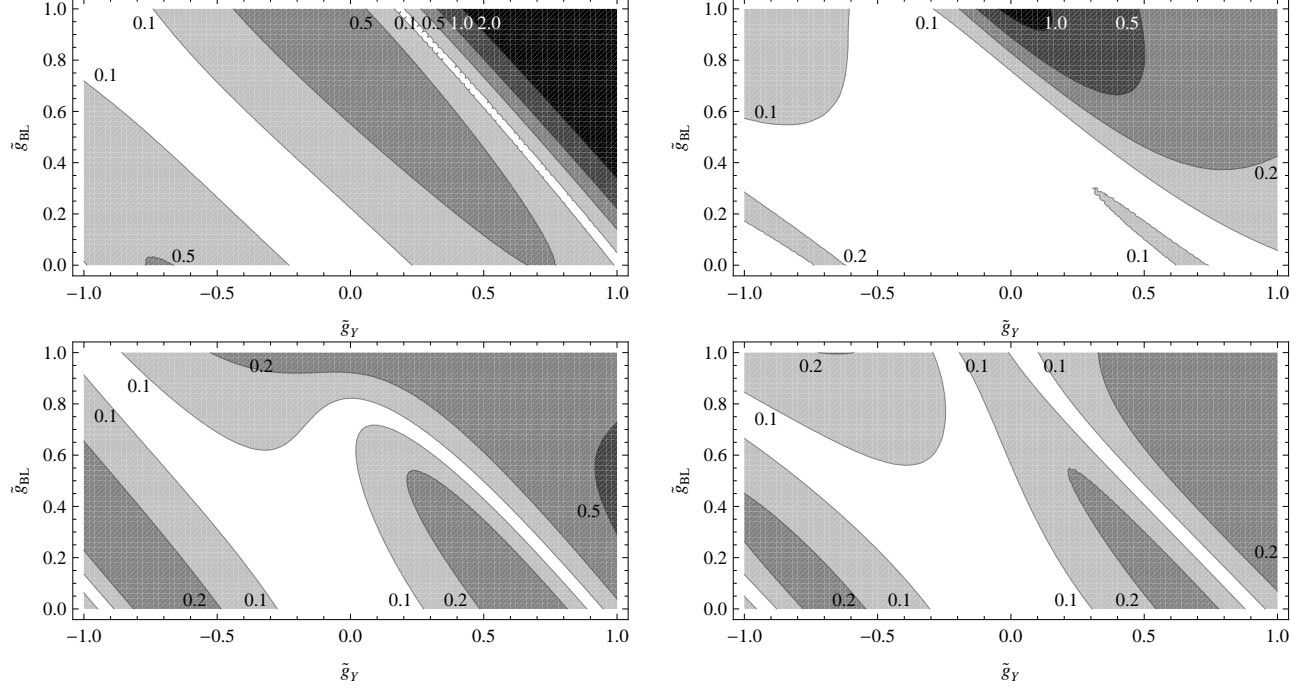


FIG. 4. Deviations with respect to the SM for  $e^+e^- \rightarrow t\bar{t}$  in the minimal  $Z'$  model at  $\sqrt{s}=3$  TeV. In the upper row we show  $|\delta\sigma|/\sigma^{SM}$  and  $|\delta A_{FB}|$ , and in the lower row the absolute value for the deviations of the polarisation-based observables  $A_{LR}$  and  $A_{FB}^{pol}$ . Darker region imply larger deviations; contour lines correspond to fixed deviation values. The middle of the X-axis corresponds to the SM.

composite fermion mass scale. By contrast with the SM case, Yukawa matrices can be chosen to be "natural", that is, with entries all of  $O(1)$ : the hierarchy in mass is created by the different values of the mixing angles. These implies that most of the mixing angles are very small, so that they are not relevant to this analysis. For our purposes, it will be sufficient to consider the fermion mass scale  $m^*$  and the Yukawa and mixing parameters relative to the third quark generation, which have to be chosen in order to satisfy the relation:

$$\frac{\sqrt{2}m_t}{v} \simeq \sin \varphi_{QL3} Y_{U33}^* \sin \varphi_{tR}, \quad \frac{\sqrt{2}m_b}{v} \simeq \sin \varphi_{QL3} Y_{D33}^* \sin \varphi_{bR}, \quad (5)$$

where  $m_t$  and  $m_b$  are the  $t$  and  $b$  mass,  $\varphi_{QL3}$ ,  $\varphi_{tR}$  and  $\varphi_{bR}$  are the mixing angles of the  $(t_L, b_L)$  doublet, the  $t_R$  and the  $b_R$  respectively, and  $Y_{U33}^*$  and  $Y_{D33}^*$  are Yukawa matrix entries.

In the present analysis, since we are interested in studying the modifications from  $Z'$  exchanges to standard four-fermion operators, we have assumed the composite fermions



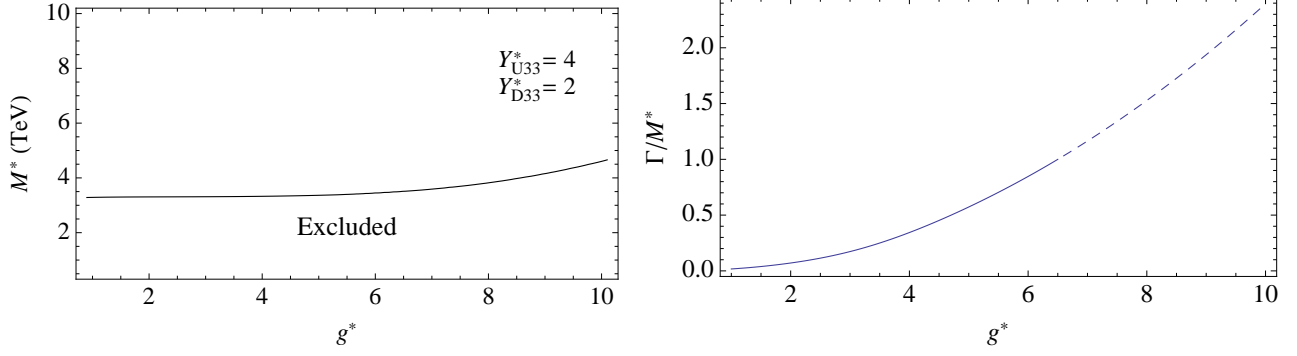


FIG. 5. On the left: allowed region for the ECHM in the  $g^*$ ,  $M^*$  plane for  $Y_{U33}^* = 4$  and  $Y_{D33}^* = 2$ , based on a 99 % C.L. fit to the S,T and U parameters and the deviation  $\delta g_{Zbb}$  of the  $Zb_L b_L$  coupling. On the right: estimate of the degree of perturbativity of the ECHM based on the rate of the width  $\Gamma$  of the broadest state (which is one of the three  $Z'$ 's), to its mass  $M^*$ . The dashed portion of the curve denotes the region in which  $\Gamma/M^* > 1$ .

mass scale,  $m^*$  to be slightly greater than  $M^* \sim m^*$  to avoid decay of the  $Z'$ 's into heavy fermions. In particular, we have chosen  $m^* = 1.5 M^*$ . For the  $3^{rd}$ -generation quarks, we have assumed, following [5], full  $t_R$  compositeness, fixing  $\sin \varphi_{UR3} = 1$ . By eq. (5), we are left with four relevant free parameters, which can be chosen to be  $Y_{U33}^*$ , the ratio  $Y_{D33}^*/Y_{U33}^*$ , the coupling  $g^*$ , and the mass scale  $M^*$ . The remaining two mixing angles are then fixed to be

$$\sin \varphi_{QL3} = \frac{\sqrt{2}m_t}{v Y_{U33}^*}, \quad \sin \varphi_{bR} = \frac{m_b}{m_t} \frac{Y_{U33}^*}{Y_{D33}^*}. \quad (6)$$

The values of  $Y_{U33}^*$  and  $Y_{D33}^*/Y_{U33}^*$  have to be chosen of order unity, and are subject to relatively strong experimental constraint since they contribute to a modification to the coupling  $Zb_L b_L$ . We have chosen to fix them to the values  $Y_{U33}^* = 4$  and  $Y_{D33}^*/Y_{U33}^* = 1/2$ , since their variation has little effect on the phenomenology for the purposes of this study.  $M^*$  has to be  $\gtrsim 3$  TeV, and  $g^*$  has to be greater than  $g_{SM} \simeq 0.65$  and not so large as to spoil the perturbativity of the model. In fig. 5 we show the constraints on the parameter space from low-energy precision observables as well as an estimate of the degree of the perturbativity based on the analysis of the width-to-mass ratio of the broadest state.

The model contains three  $Z'$  bosons, originating from the  $SU(2)_L \otimes SU(2)_L \otimes U(1)_X$  composite subsector. They are nearly degenerate by construction, all three having mass of order  $M^*$ . Their couplings to fermions depend strongly on the fermion mixing angle; for the

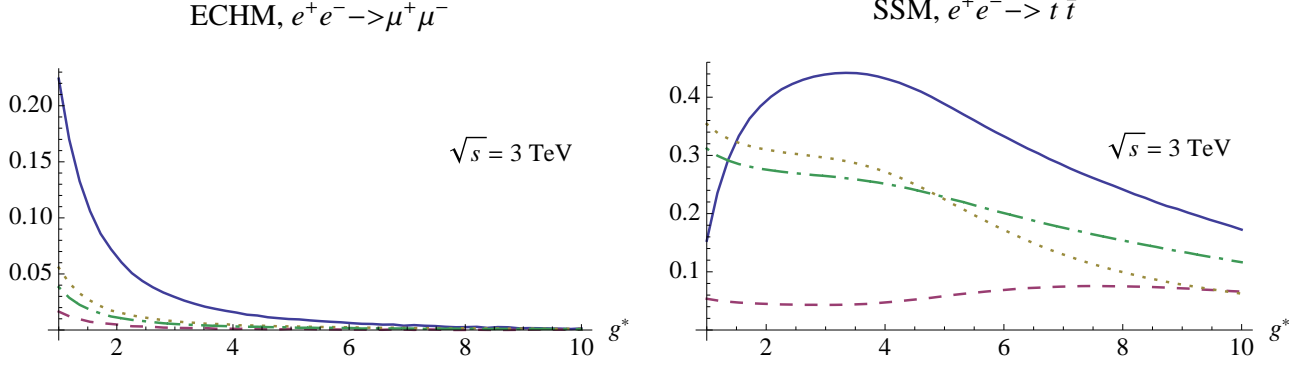


FIG. 6. Deviations with respect to the SM for  $e^+e^- \rightarrow \mu^+\mu^-$  (left) and to  $e^+e^- \rightarrow t\bar{t}$  (right) in the ECHM at  $\sqrt{s}=3$  TeV with the mass scale fixed at  $M^* = 5$  TeV and  $Y_{U33}^* = 4$ ,  $Y_{D33}^* = 2$ . The continuous line represents the relative cross-section deviation  $\delta\sigma/\sigma^{SM}$ ; the dashed line gives  $\delta A_{FB}$ , the dotted line  $\delta A_{LR}$  and the dot-dashed line  $\delta A_{FB}^{pol}$ .

(chiral) fermion  $f$  they are generically of order

$$g_{Z'}^f \simeq g \left( \frac{g^*}{g} \sin^2 \varphi_f - \frac{g}{g^*} \cos^2 \varphi_f \right), \quad (7)$$

where  $g$  is a generic SM coupling. Since for every fermion except the third generation quarks the mixing angle is very small, by eq. (7) the corresponding couplings are suppressed by factors  $g/g^*$  and are smaller than the SM values; this is also true for  $b_R$  (see eq. (6)). The situation is opposite for the  $t_R$ , which has  $\varphi_{tR} = 1$  implying a coupling of order  $g^*$ . The left-handed third generation quarks  $t_L$  and  $b_L$  are in an intermediate situation, with a mixing angle approximately equal to  $1/Y_{U33}^*$ . However, since their coupling depend on two contributions of opposite sign, they are in general not significantly enhanced with respect to the SM ones. In the end, the best sensitivity is expected in the top channel. As we show in fig. 6, this is indeed the case, especially as  $g^*$  grows to be larger than  $\sim 2$ . Again, deviations can be very significant, and the sensitivity extends well beyond 10 TeV.

### C. Conclusions

We have examined the phenomenology of two different physical scenarios, both including  $Z'$ s, at a linear collider when the mass scale of the new physics is beyond the direct reach of the collider, by looking at precision observables on  $e^+e^- \rightarrow f\bar{f}$  processes for  $f = \mu, t$ . In the first case, the minimal  $Z'$  model [3], which describes a “typical”  $Z'$  scenario, we found

similar deviations from the SM predictions in both fermion channels. In the case of the ECHM model which is based on the presence of a composite sector at the TeV scale, we found that deviations in the muon channel are generally suppressed, while those in the top channel are enhanced. In both cases deviations are sizable and the sensitivity may extend to very high mass scales depending on experimental conditions. Furthermore the very different observable behaviour in the two scenarios can let us distinguish them even if no direct signal is observed.

## ACKNOWLEDGMENTS

The authors wish to thank R. Contino for useful discussions regarding the ECHM model. We also thank E. Boos and S. Bunichev for advice on how to implement beam polarisation in CompHEP/CalcHEP.

- 
- [1] G. Aad *et al.* [ATLAS Collaboration], Phys. Rev. Lett. **107** (2011) 272002 [arXiv:1108.1582 [hep-ex]].
  - [2] [CMS Collaboration], CMS-PAS-EXO-11-019.
  - [3] T. Appelquist, B. A. Dobrescu and A. R. Hopper, Phys. Rev. D **68** (2003) 035012 [arXiv:hep-ph/0212073].
  - [4] E. Salvioni, G. Villadoro, F. Zwirner, JHEP **0911** (2009) 068. [arXiv:0909.1320 [hep-ph]]
  - [5] R. Contino, T. Kramer, M. Son *et al.*, JHEP **0705** (2007) 074. [hep-ph/0612180]
  - [6] A. Pukhov, [hep-ph/0412191]
  - [7] N. D. Christensen and C. Duhr, Comput. Phys. Commun. **180**, 1614 (2009) [arXiv:0806.4194 [hep-ph]].
  - [8] Mathematica is a trademark of Wolfram Research Inc.
  - [9] S. Jadach, B. F. L. Ward, Comput. Phys. Commun. **56** (1990) 351-384;  
M. Skrzypek, S. Jadach, Z. Phys. **C49** (1991) 577-584.
  - [10] G. Moortgat-Pick *et al.*, Phys. Rept. **460**, 131 (2008) [arXiv:hep-ph/0507011].
  - [11] [CLIC Collaboration], CLIC CDR, in publication
  - [12] S. Riemann, In \*2nd ECFA/DESY Study 1998-2001\* 1451-1468.

- [13] K. Agashe, A. Delgado, M. J. May *et al.*, JHEP **0308** (2003) 050. [hep-ph/0308036]
- [14] K. Agashe, R. Contino, L. Da Rold and A. Pomarol, Phys. Lett. B **641**, 62 (2006) [arXiv:hep-ph/0605341].